Spin-charge coupling and the high-energy magnetodielectric effect in hexagonal $HoMnO_3$

R. C. Rai,[1] J. Cao,[1] J. L. Musfeldt,[1] S. B. Kim,[2] S.-W. Cheong,[2] and X. Wei[3]
[1]*Department of Chemistry, University of Tennessee, Knoxville, Tennessee 37996, USA*
[2]*Rutgers Center for Emergent Materials and Department of Physics and Astronomy, Rutgers University, Piscataway, New Jersey 08854, USA*
[3]*National High Magnetic Field Laboratory, Florida State University, Tallahassee, Florida 32310, USA*
(Received 11 December 2006; revised manuscript received 26 February 2007; published 15 May 2007)

We investigate the optical and magneto-optical properties of $HoMnO_3$ in order to elucidate the spin-charge coupling and high-energy magnetodielectric effect. We find that the Mn *d* to *d* excitations are sensitive to the cascade of low-temperature magnetic transitions involving the Mn^{3+} moment, direct evidence for spin-charge coupling. An applied magnetic field also modifies the on-site excitations. The high-energy magnetodielectric contrast (~8% at 20 T near 1.8 eV) derives from the substantial mixing in this multiferroic system.

DOI: 10.1103/PhysRevB.75.184414 PACS number(s): 75.80.+q, 75.50.Ee, 78.20.Ls, 78.20.Ci

I. INTRODUCTION

$RMnO_3$ manganites (R=rare earth) are flexible frameworks for the development of novel functional materials. They have attracted recent attention due to the fundamental physics underlying the coexistence of ferroelectric and antiferromagnetic orders, an effect that, although rare, is very promising for device applications.[1–9] $HoMnO_3$ is a prototype of this family of materials and has been extensively studied in both its hexagonal and orthorhombic forms.[9–16] Static (kilohertz) magnetodielectric measurements are particularly exciting because magnetoelectric coupling allows for the tuning of dielectric properties with an applied magnetic field.[15,17–19] The recent discovery of ferroelectricity in orthorhombic $HoMnO_3$ is another stunning example of the magnetoelectric effect.[20,21] The coupling between ferroelectric and antiferromagnetic order parameters in $HoMnO_3$ has not been unambiguously explained, although Ho-Mn exchange and anisotropy interactions,[12] spin-phonon coupling,[18,22] and possible Dzyaloshinskii-Moriya interactions[20,23,24] have been invoked. Direct measurements of spin-charge interaction are therefore needed to provide microscopic insight into the coupling process. Further, the high-energy magnetodielectric effect, reported recently in other layered transition-metal oxides,[25,26] is unexplored in the rare-earth manganites.

Figure 1(a) displays the quasihexagonal crystal structure of $HoMnO_3$ at 300 K.[27] It consists of layers of corner sharing MnO_5 trigonal bipyramids, separated by layers of Ho^{3+} ($4f^{10}$) ions. Each unit cell contains six formula units and two layers of slightly distorted MnO_5 trigonal bipyramids in which the Mn^{3+} ($3d^4$) ions are located near the center. Below the ferroelectric transition temperature (T_{FE}~900 K), the Mn^{3+} spins and the associated magnetic exchange are confined to the basal (*ab*) plane, and Mn^{3+} spins are geometrically frustrated due to the quasitriangular lattice. The ferroelectric moment along the *c* axis in this phase is due to Ho-O displacements that occur at T_{FE}.[12] With decreasing temperature, $HoMnO_3$ exhibits a cascade of magnetic transitions that arise primarily from Mn^{3+} and Ho^{3+} spin orderings.[2,12,17–19] Ferroelectric and antiferromagnetic orders coexist below the Néel temperature (T_N~75 K), where Mn^{3+} spins order antiferromagnetically.[28] This magnetic ordering affects both Raman and infrared-active Mn-O-Mn phonons.[22] The Mn^{3+} spins reorient further at T_{SR} (~42 K) by rotating 90° within the basal plane.[17] Interactions involving rare-earth spin centers are responsible for the lowest-temperature phases at zero field. Some Ho^{3+} spins order antiferromagnetically along the *c* axis at ~8 K, whereas the other Ho^{3+} spins remain in the paramagnetic state down to 1.7 K.[10] Application of a magnetic field reveals a rich *H-T* phase diagram. At this time, at least six different magnetic phases have been reported.[19] In particular, the external magnetic field can access three distinct phases ($P6_3cm$, $P6_3$, and $P6_3cm$) in the ~5–35 K temperature range.[17–19,29] The critical fields associated with these phases can vary, depending on the temperature. In the $P6_3$ phase, the Mn^{3+} moments lie at an intermediate angle between 0° and 90° with respect to the *a* axis, and a small hysteresis effect has been reported.[19,28]

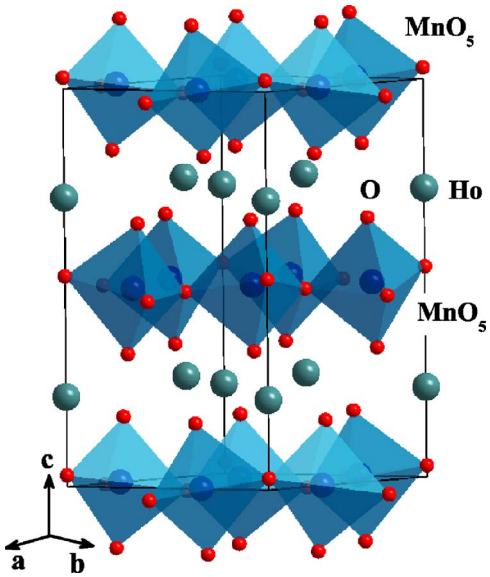

FIG. 1. (Color online) 300 K crystal structure of $HoMnO_3$ showing layers of distorted MnO_5 bipyramidal building block units separated by layers of Ho^{3+} ions (Refs. 10 and 27). Shading of the MnO_5 bipyramids indicates tilting with respect to the *c* axis. $HoMnO_3$ displays a $P6_3cm$ space group at 300 K.

In order to investigate spin-charge coupling and the high-energy magnetodielectric effect in a frustrated multiferroic, we measured the optical and magneto-optical properties of hexagonal $HoMnO_3$. We find that the Mn d to d excitations are sensitive to the cascade of low-temperature magnetic transitions involving the Mn^{3+} moment, direct evidence for spin-charge coupling. An applied magnetic field also modifies the Mn d to d on-site excitations. The high-energy magnetodielectric contrast (~8% at 20 T near 1.8 eV) derives from the substantial spin-lattice-charge coupling and is comparable to that found in mixed-valent $K_2V_3O_8$ and the frustrated Kagomé lattice compound $Ni_3V_2O_8$.[25,26] The high-energy magnetodielectric contrast in quasihexagonal $HoMnO_3$ is similar in size to the static dielectric effect,[17–19] a rather unexpected finding considering the substantially different energy scales.

II. METHODS

Single crystals of $HoMnO_3$ were grown using a traveling solvent optical floating zone technique and characterized by magnetization, polarization, and x-ray diffraction. Samples were cut to expose the (001) face, and an optically smooth surface was prepared by polishing. Typical crystal dimensions were $3\times3\times2$ mm^3.

Near normal *ab*-plane reflectance of $HoMnO_3$ was measured over a wide energy range (65 meV–6.5 eV) using a Bruker Equinox 55 Fourier transform infrared spectrometer equipped with an infrared microscope and a Perkin Elmer Lambda-900 grating spectrometer. The spectral resolution was 2 cm^{-1} in the middle infrared and 2 nm in the near infrared, visible, and near ultraviolet. Optical conductivity was extracted by a Kramers-Kronig analysis of the measured reflectance.[30] An open flow cryostat and a temperature controller were used for variable-temperature studies. Standard peak-fitting techniques were used, as appropriate.

The magneto-optical properties of $HoMnO_3$ were investigated between 0.75 and 4.1 eV using a 3/4 m grating spectrometer equipped with InGaAs and charge-coupled device detectors and a 33 T resistive magnet at the National High Magnetic Field Laboratory, Tallahassee, FL.[25] Experiments were performed at 6, 20, and 45 K for $H\|c$. The field-induced changes in the measured reflectance were analyzed by taking the ratio of reflectance at each field and reflectance at zero field, i.e., $[R(H)/R(H=0\text{ T})]$. Such a normalized response highlights the field-induced optical changes.[31] The high-field optical conductivity (σ_1) and dielectric response (ϵ_1) were extracted by renormalizing the zero-field absolute reflectance with the high-field reflectance ratios and recalculating the optical properties using Kramers-Kronig techniques.[25,30] Recall that $\epsilon(E)=\epsilon_1(E)+i\epsilon_2(E)$. Optical conductivity $\sigma_1(E)$ is proportional to the lossy part of the dielectric function. To facilitate comparison with static magnetodielectric measurements, we define the magnetodielectric contrast as $[\epsilon_1(E,H)-\epsilon_1(E,0)]/\epsilon_1(E,0)=\Delta\epsilon_1/\epsilon_1$. We also define the dielectric contrast with respect to temperature as $[\epsilon_1(E,T_2)-\epsilon_1(E,T_1)]/\epsilon_1(E,T_1)=\Delta\epsilon_1/\epsilon_1$.

III. RESULTS AND DISCUSSION

Figure 2 displays the *ab*-plane optical conductivity of

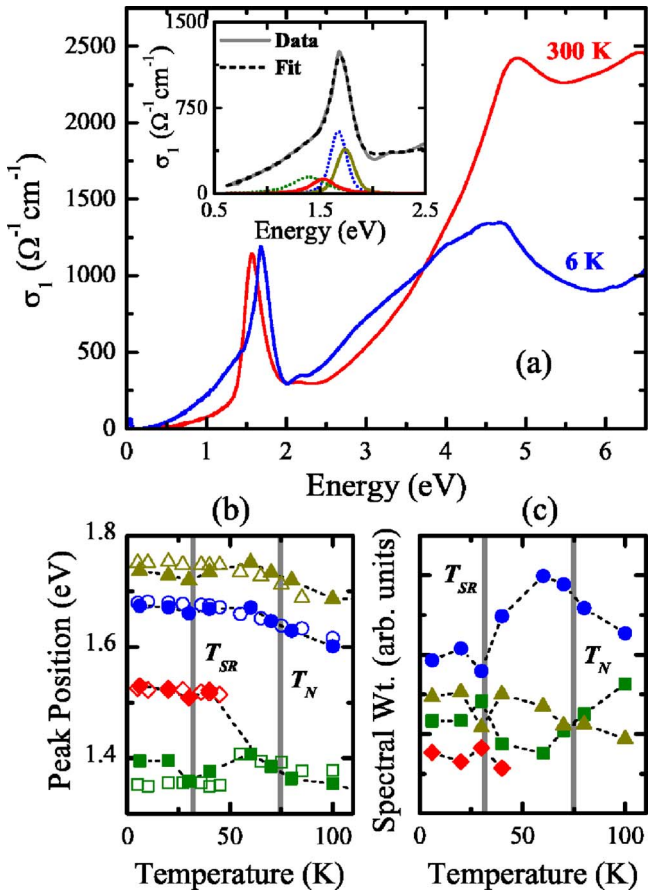

FIG. 2. (Color online) (a) *ab*-plane optical conductivity of $HoMnO_3$ at 300 and 6 K extracted from the measured reflectance by a Kramers-Kronig analysis. The inset shows a typical peak fit of the Mn d to d band at 6 K. (b) Peak positions of model oscillators, fitted to the on-site excitations, as a function of temperature. Open and closed symbols represent the two sets of independently measured data. Error bars in the fit are on the order of the symbol size. The shaded vertical lines designate the well-known T_N and T_{SR} transitions. (c) Spectral weight of model oscillators as a function of temperature. The symbols in this panel correspond to those in panel (b).

$HoMnO_3$ at 300 and 6 K. The spectra show several strong electronic excitations and an optical gap of ~0.5 eV. Based on comparison with chemically similar Mn-containing compounds,[32,33] we assign the peak centered near ~1.7 eV to Mn d to d on-site excitations. These excitations are optically allowed due to the low symmetry of the local environment and hybridization between the Mn d and O p states. Second-harmonic generation and time-resolved third-order nonlinear optical spectroscopies on this family of manganites support this assignment.[9,34,35] An alternate view of the electronic structure has also been proposed.[36–38] Within this interpretation, the ~1.7 eV peak corresponds to a charge-transfer gap deriving from O p to Mn d excitations. Based on the surprisingly large value of on-site electron correlation employed in the electronic structure calculations, the fact that the calculated optical spectrum employing $U=8$ eV does not resemble the data in Fig. 2,[36] and the challenge of getting a neutral surface cleavage plane for photoemission studies,[38]

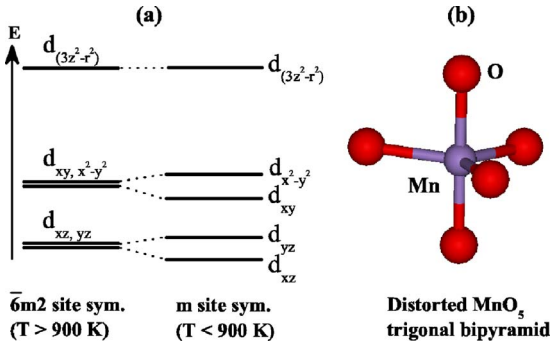

FIG. 3. (Color online) (a) Schematic symmetry decent diagram showing the crystal-field splitting of the Mn^{3+} d levels in the high-temperature paraelectric state and the splitting of these energy levels due to the reduced site symmetry around the Mn^{3+} center below T_{FE}. (b) Distorted MnO_5 trigonal bipyramid building block unit highlighting the reduced local symmetry around the Mn^{3+} center.

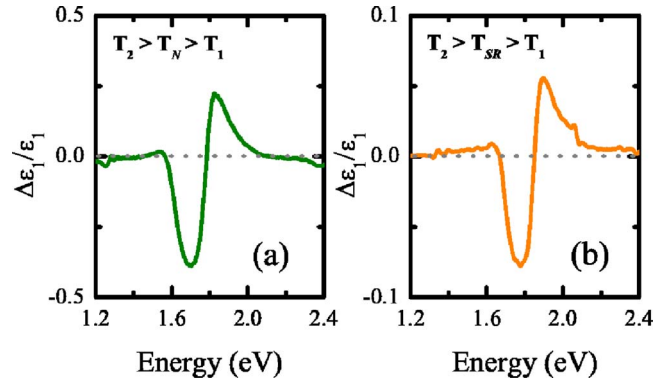

FIG. 4. (Color online) The high-energy dielectric contrast $\Delta\epsilon_1/\epsilon_1$ of $HoMnO_3$ in the region of the Mn d to d excitations (a) for T_2=85 K, T_1=65 K ($T_2 > T_N > T_1$) and (b) for T_2=45 K, T_1 =30 K ($T_2 > T_{SR} > T_1$).

the picture of $HoMnO_3$ as a charge-transfer insulator seems more controversial. Assigning the ~1.7 eV peak to on-site excitations, the asymmetric shape derives from crystal-field splitting of the d manifold and the consequent overlap of the different excitations. This band changes with temperature, as discussed below. The ~3 and 4.5 eV features derive from O $2p$ to Mn $3d$ charge transfer excitations.

Below T_{FE}, a distortion around the Mn^{3+} centers breaks the local bipyramidal symmetry, and the doubly degenerate transition-metal d levels are split. This symmetry reduction is shown schematically in Fig. 3. Since the d_{xz}, d_{yz}, d_{xy}, and $d_{x^2-y^2}$ levels are close in energy even in this reduced symmetry phase, Hund's rule of maximum multiplicity favors the high-spin state (S=2) for Mn^{3+}. As a consequence, four unique on-site excitations are allowed within the transition-metal d manifold. These excitations are formally allowed by symmetry in a distorted bipyramidal environment, even in the absence of hybridization with oxygen. We can compare these simple crystal-field predictions with the measured optical spectra [Fig. 2(a)]. At 300 K, the ~1.7 eV feature is sharp and slightly asymmetric. It broadens substantially at low temperatures, a signature of multiple overlapping Mn d to d excitations.[39]

In order to extract quantitative information on temperature-driven changes within the Mn d manifold, we fitted the optical spectra in this region with several model Voigt oscillators [inset, Fig. 2(a)]. At high temperatures, the ~1.7 eV feature can be modeled with two Voigt oscillators, whereas at low temperatures, four oscillators are required. That only two oscillators are needed to mimic the 300 K spectrum indicates the importance of linewidth broadening effects. That four oscillators capture the low-temperature response is in accord with the expected excitation profile for a distorted MnO_5 trigonal bipyramid building block in the ferroelectric phase.

Excitations within the d manifold of complex oxides are known to be sensitive to the local crystal-field environment.[25,33,35,40] They can also be sensitive to magnetic order if the charge, lattice, and spin channels are coupled.[13,41,42] Figure 2(b) displays the peak positions obtained from the aforementioned model oscillator analysis (corresponding to the various Mn d to d on-site excitations) as a function of temperature. The peak positions of fitted oscillators display anomalies at ~75 and 35 K, in excellent agreement with the well-known T_N (antiferromagnetic) and T_{SR} (Mn^{3+} spin rotation) transitions in $HoMnO_3$. The spectral weights, obtained by integrating the optical conductivity between 0.6 and 2.5 eV, of the model oscillators also show anomalies at T_N and T_{SR} [Fig. 2(c)]. Within our sensitivity, the Mn d to d on-site excitations are not affected by the 8 K Ho^{3+} ordering. The correlation between the various components of the Mn d to d excitations (represented by the four model oscillators) and the magnetic transitions involving Mn^{3+} moment demonstrates that charge excitations are sensitive to the magnetic order and symmetry, providing direct evidence for spin-charge coupling in this frustrated multiferroic material. We anticipate that f manifold excitations will display coupling to the 8 and 1.7 K transitions involving Ho^{3+} spins.[22]

The dielectric properties also change significantly through the magnetic transitions. Figure 4 shows the dielectric contrast of $HoMnO_3$, $\Delta\epsilon_1/\epsilon_1$, around T_N and T_{SR}. The dielectric contrast is large: ~40% near 1.7 eV around T_N and ~8% near 1.8 eV around T_{SR}.[43] Based on the position of these features, the dielectric contrast in $HoMnO_3$ is associated with dispersive changes in the Mn d to d on-site excitations, with the highest-energy d_{xz} to $d_{(3z^2-r^2)}$ and d_{yz} to $d_{(3z^2-r^2)}$ excitations being most strongly affected. We therefore see that the spin-charge coupling depends on symmetry. Dielectric changes are also observed at 90 K in $LuMnO_3$.[33] Together, these results demonstrate that high-energy dielectric contrast can be achieved by physical tuning through the magnetic transitions in well-coupled materials.

Given the evidence for substantial mixing in $HoMnO_3$, we extended our work to include high-field magneto-optical measurements. Figure 5(a) shows the reflectance ratio, $R(H)/R(H=0\ \mathrm{T})$, of $HoMnO_3$ at 6 K. At 20 T, the reflectance decreases by ~1.5% near 1.8 eV. The effect is smaller at higher temperatures.[44] To correlate field-induced changes in reflectance with the optical constants, we combined these results with absolute reflectance measurements and a Kramers-Kronig analysis to extract the optical conductivity

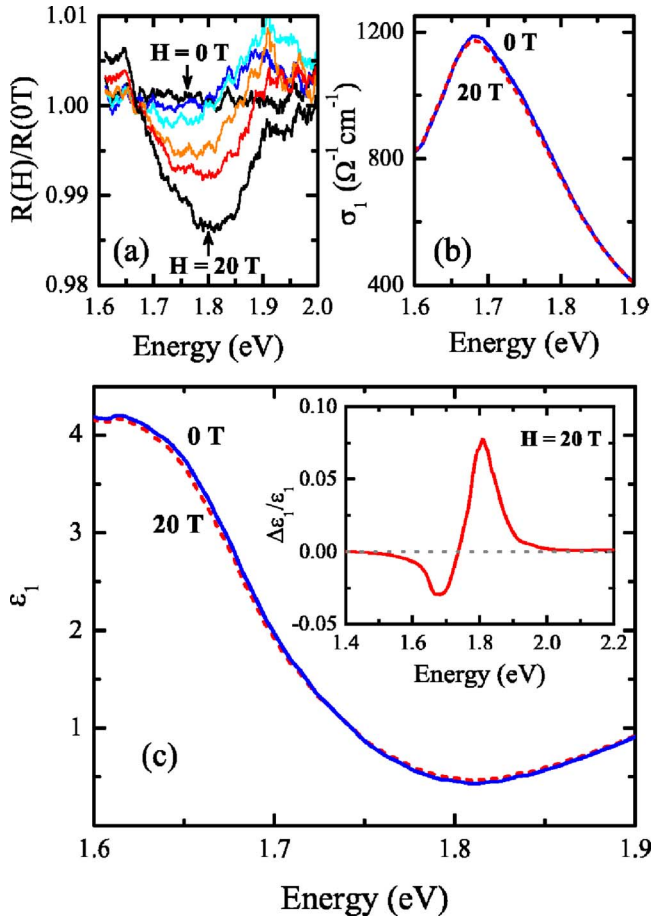

FIG. 5. (Color online) (a) The 6 K normalized magneto-optical response of $HoMnO_3$, $R(H)/R(H=0\ \mathrm{T})$, in an applied magnetic field from 0 to 20 T ($H \| c$). Data are shown in 4 T steps. (b) *ab*-plane optical conductivity for $H=0$ (solid line) and 20 T (dashed line) ($H \| c$) at 6 K. (c) Dielectric response for $H=0$ (solid line) and 20 T (dashed line) ($H \| c$) at 6 K. The inset shows a close-up view of the high-energy dielectric contrast, $\Delta\epsilon_1/\epsilon_1$, which is the largest in the region of the Mn *d* to *d* excitations.

and dielectric response. Field-induced modifications of σ_1 and ϵ_1 further our understanding of the magnetodielectric effect in complex materials.

Figure 5(b) shows a close-up view of the optical conductivity of $HoMnO_3$ at 0 and 20 T. The observed magneto-optical response correlates directly with a field-induced narrowing of the Mn *d* to *d* color band excitation. The reflectance ratio changes also yield field-dependent dielectric properties. Figure 5(c) shows a close-up view of the real part of the dielectric constant of $HoMnO_3$ at 0 and 20 T. The dispersive shape of ϵ_1 in this region is associated with the aforementioned Mn *d* to *d* excitations. The inset in Fig. 5(c) displays the high-energy magnetodielectric contrast $\Delta\epsilon_1/\epsilon_1$ at 20 T. The size of the dielectric contrast depends on energy and is as large as ~8% at 20 T near 1.8 eV. It can be either positive or negative depending on the energy, again demonstrating appreciable interplay between the electronic and magnetic properties in this material. The dielectric contrast is much larger than that expected based on simple energy scale arguments.

The high-energy magnetodielectric effect in $HoMnO_3$ is small at low fields, becomes appreciable only above 10 T (in the $P6_3cm$ phase), and reaches ~8% at 20 T near 1.8 eV. This is surprisingly similar in size to the static magnetodielectric response of hexagonal $HoMnO_3$, which is ~2%–3% at low fields.[17–19] The authors of Refs. 17–19 attribute the static magnetodielectric contrast to spin-phonon coupling effects. Variable-temperature infrared studies support this conclusion, revealing anomalies in two-phonon modes near the magnetic ordering temperature (T_N), direct evidence for strong coupling.[22] Isostructural $LuMnO_3$ also has two low-frequency phonons that display strong absolute frequency shifts and inflection points at T_N.[33] Mixing between phonons and electromagnons has recently been observed in $GdMnO_3$.[45]

The high-energy dielectric contrast in $HoMnO_3$ (~8% at 20 T near 1.8 eV) is similar to that observed in other complex oxides such as inhomogeneously mixed-valent $K_2V_3O_8$ (~5% at 30 T near 1.2 eV)[25] and Kagomé staircase compound $Ni_3V_2O_8$ (~16% at 30 T near 1.3 eV).[26] For both $K_2V_3O_8$ and $Ni_2V_2O_8$, the largest field-induced changes are observed in the vicinity of the transition-metal *d* to *d* excitations, although smaller field-induced structures are present in the bands associated with O *p* to transition-metal *d* charge-transfer excitations.[25,26] In contrast, $HoMnO_3$ does not display any field-induced changes in the O *p* to Mn *d* charge-transfer bands.[46] For $K_2V_3O_8$, the demonstrably soft lattice favors magnetoelastic coupling, driving the high-energy magnetodielectric effect.[25] For $HoMnO_3$ and $Ni_3V_2O_8$, combined lattice and magnetic frustration effects seem to be important. The molecular magnet Ni_4Mo_{12} provides another point of comparison. Here, the high-energy dielectric contrast is much smaller (~0.5% at 30 T near 1.9 eV),[31] and direct measurements show that the lattice coupling is weak.[47] We conclude that intermediate coupling is favorable for the high-energy magnetodielectric effect.

IV. CONCLUSION

We report the optical and magneto-optical properties of $HoMnO_3$ in order to investigate the high-energy magnetodielectric effect and to elucidate the interplay between spin and charge degrees of freedom in a frustrated low-dimensional multiferroic. The Mn *d* to *d* excitations are very sensitive to the cascade of low-temperature magnetic transitions. This is because the local environment around the Mn^{3+} center is subtly modified at T_{SR} and T_N. This sensitivity provides direct evidence of spin-charge coupling, complementing the comprehensive vibrational properties work of Ref. 22. Given the evidence for substantial mixing in $HoMnO_3$, we extended these studies to include high-field magneto-optical spectroscopies. Field-induced optical property modifications are observed in the region of the Mn *d* to *d* excitations. We find that the high-energy magnetodielectric contrast in $HoMnO_3$ is ~8% at 20 T near 1.8 eV, similar in magnitude to that in

the frustrated Kagomé lattice compound $Ni_3V_2O_8$ (~16% at 30 T near 1.3 eV) and the mixed-valent magnetic oxide $K_2V_3O_8$ (~5% at 30 T near 1.2 eV). The magnetodielectric contrast in $HoMnO_3$ can be positive or negative depending on the energy. The importance of intermediate coupling was advanced in the past for both $Ni_3V_2O_8$ and $K_2V_3O_8$ and may provide the key to the development of tunable magnetically controlled ferroelectric memory. The relationship between the static and high-energy magnetodielectric effects in $HoMnO_3$ is also discussed.

ACKNOWLEDGMENTS

Work at the University of Tennessee is supported by the Materials Science Division, Basic Energy Sciences, U.S. Department of Energy (DE-FG02-01ER45885). Research at Rutgers University is supported by the National Science Foundation (DMR-0520471). A portion of this research was performed at the NHMFL, which is supported by NSF Cooperation Agreement DMR-0084173 and by the State of Florida. We thank David Singh for useful discussions.

[1] Z. J. Huang, Y. Cao, Y. Y. Sun, Y. Y. Xue, and C. W. Chu, Phys. Rev. B **56**, 2623 (1997).
[2] M. Fiebig, T. Lottermoser, D. Fröhlich, A. V. Goltsev, and R. V. Pisarev, Nature (London) **419**, 818 (2002).
[3] A. Muñoz, J. A. Alonso, M. J. Martínez-Lope, M. T. Casáis, J. L. Martínez, and M. T. Fernández-Díaz, Phys. Rev. B **62**, 9498 (2000).
[4] T. Katsufuji, S. Mori, M. Masaki, Y. Moritomo, N. Yamamoto, and H. Takagi, Phys. Rev. B **64**, 104419 (2001).
[5] B. B. Van Aken, T. T. M. Palstra, A. Filippetti, and N. A. Spaldin, Nat. Mater. **3**, 164 (2004).
[6] T. Lonkai, D. G. Tomuta, U. Amann, J. Ihringer, R. W. A. Hendrikx, D. M. Többens, and J. A. Mydosh, Phys. Rev. B **69**, 134108 (2004).
[7] T. Lottermoser and M. Fiebig, Phys. Rev. B **70**, 220407(R) (2004).
[8] P. A. Sharma, J. S. Ahn, N. Hur, S. Park, S. B. Kim, S. Lee, J.-G. Park, S. Guha, and S.-W. Cheong, Phys. Rev. Lett. **93**, 177202 (2004).
[9] M. Fiebig, D. Fröhlich, K. Kohn, S. Leute, T. Lottermoser, V. V. Pavlov, and R. V. Pisarev, Phys. Rev. Lett. **84**, 5620 (2000).
[10] A. Muñoz, J. A. Alonso, M. J. Martínez-Lope, M. T. Casáis, J. L. Martínez, and M. T. Fernández-Díaz, Chem. Mater. **13**, 1497 (2001).
[11] T. Lottermoser, T. Lonkai, U. Amann, D. Hohlwein, J. Ihringer, and M. Fiebig, Nature (London) **430**, 541 (2004).
[12] O. P. Vajk, M. Kenzelmann, J. W. Lynn, S. B. Kim, and S.-W. Cheong, Phys. Rev. Lett. **94**, 087601 (2005).
[13] C. dela Cruz, F. Yen, B. Lorenz, Y. Q. Wang, Y. Y. Sun, M. M. Gospodinov, and C. W. Chu, Phys. Rev. B **71**, 060407(R) (2005).
[14] H. W. Brinks, J. Rodríguez-Carvajal, H. Fjellvåg, A. Kjekshus, and B. C. Hauback, Phys. Rev. B **63**, 094411 (2001).
[15] B. Lorenz, Y. Q. Wang, Y. Y. Sun, and C. W. Chu, Phys. Rev. B **70**, 212412 (2004).
[16] J. S. Zhou, J. B. Goodenough, J. M. Gallardo-Amores, E. Moran, M. A. Alario-Franco, and R. Caudillo, Phys. Rev. B **74**, 014422 (2006).
[17] B. Lorenz, A. P. Litvinchuk, M. M. Gospodinov, and C. W. Chu, Phys. Rev. Lett. **92**, 087204 (2004).
[18] B. Lorenz, F. Yen, M. M. Gospodinov, and C. W. Chu, Phys. Rev. B **71**, 014438 (2005).
[19] F. Yen, C. R. dela Cruz, B. Lorenz, Y. Y. Sun, Y. Q. Wang, M. M. Gospodinov, and C. W. Chu, Phys. Rev. B **71**, 180407(R) (2005).
[20] I. A. Sergienko, C. Şen, and E. Dagotto, Phys. Rev. Lett. **97**, 227204 (2006).
[21] B. Lorenz, Y. Q. Wang, and C. W. Chu, arXiv:cond-mat/0608195 (unpublished).
[22] A. P. Litvinchuk, M. N. Iliev, V. N. Popov, and M. M. Gospodinov, J. Phys.: Condens. Matter **16**, 809 (2004).
[23] H. Katsura, N. Nagaosa, and A. V. Balatsky, Phys. Rev. Lett. **95**, 057205 (2005).
[24] I. A. Sergienko and E. Dagotto, Phys. Rev. B **73**, 094434 (2006).
[25] R. C. Rai, J. Cao, J. L. Musfeldt, D. J. Singh, X. Wei, R. Jin, Z. X. Zhou, B. C. Sales, and D. Mandrus, Phys. Rev. B **73**, 075112 (2006).
[26] R. C. Rai, J. Cao, S. Brown, J. L. Musfeldt, D. Kasinathan, D. J. Singh, G. Lawes, N. Rogado, R. J. Cava, and X. Wei, Phys. Rev. B **74**, 235101 (2006).
[27] H. L. Yakel, W. C. Koehler, E. F. Bertaut, and E. F. Forrat, Acta Crystallogr. **16**, 957 (1963).
[28] M. Fiebig, C. Degenhardt, and R. V. Pisarev, J. Appl. Phys. **91**, 8867 (2002).
[29] T. Lonkai, D. Hohlwein, J. Ihringer, and W. Prandl, Appl. Phys. A: Mater. Sci. Process. **74**, S843 (2002).
[30] F. Wooten, *Optical Properties of Solids* (Academic, New York, 1972).
[31] J. Schnack, M. Brüger, M. Luban, P. Kögerler, E. Morosan, R. Fuchs, R. Modler, H. Nojiri, R. C. Rai, J. Cao, J. L. Musfeldt, and X. Wei, Phys. Rev. B **73**, 094401 (2006).
[32] J. E. Medvedeva, V. I. Anisimov, M. A. Korotin, O. N. Mryasov, and A. J. Freeman, J. Phys.: Condens. Matter **12**, 4947 (2000).
[33] A. B. Souchkov, J. R. Simpson, M. Quijada, H. Ishibashi, N. Hur, J. S. Ahn, S.-W. Cheong, A. J. Millis, and H. D. Drew, Phys. Rev. Lett. **91**, 027203 (2003).
[34] D. Fröhlich, St. Leute, V. V. Pavlov, and R. V. Pisarev, Phys. Rev. Lett. **81**, 3239 (1998).
[35] A. V. Kimel, R. V. Pisarev, F. Bentivegna, and T. Rasing, Phys. Rev. B **64**, 201103(R) (2001).
[36] M. Qian, J. Dong, and D. Y. Xing, Phys. Rev. B **63**, 155101 (2001).
[37] A. M. Kalashnikova and R. V. Pisarev, JETP Lett. **78**, 143 (2003).
[38] J.-S. Kang, S. W. Han, J.-G. Park, S. C. Wi, S. S. Lee, G. Kim, H. J. Song, H. J. Shin, W. Jo, and B. I. Min, Phys. Rev. B **71**, 092405 (2005).
[39] Because the d_{xz}/d_{yz} and $d_{xy}/d_{x^2-y^2}$ pairs are close together, two excitations are observed at high temperatures due to linewidth broadening effects, but four independent excitations are resolved at low temperatures.

[40] H. Sawada, Y. Morikawa, K. Terakura, and N. Hamada, Phys. Rev. B **56**, 12154 (1997).

[41] S. Lee, A. Pirogov, J. H. Han, J.-G. Park, A. Hoshikawa, and T. Kamiyama, Phys. Rev. B **71**, 180413(R) (2005).

[42] M. A. Quijada, J. R. Simpson, L. Vasiliu-Doloc, J. W. Lynn, H. D. Drew, Y. M. Mukovskii, and S. G. Karabashev, Phys. Rev. B **64**, 224426 (2001).

[43] This is much larger than expected due to simple temperature effects.

[44] At 20 K, the magneto-optical response is very small in the $P6_3cm$ and $P6_3$ phases, becoming detectable only in the $P6_3cm$ phase. The magneto-optical response disappears at 45 K.

[45] A. Pimenov, T. Rudolf, F. Mayr, A. Loidl, A. A. Mukhin, and A. M. Balbashov, Phys. Rev. B **74**, 100403(R) (2006).

[46] The lack of field dependence to the higher-energy charge-transfer excitations is another argument in favor of our assignment of the ~1.7 eV feature in the optical conductivity as *d* to *d* on-site excitations rather than it being charge transfer in origin.

[47] J. Cao, R. C. Rai, J. L. Musfeldt, Y. J. Wang, M. Pederson, R. Klemm, M. Luban, and P. Kögerler (unpublished).